Supplementary Material

for

Impact of wind on crash-landing mortality in grey-headed albatrosses *Thalassarche chrysostoma* breeding on Marion Island

Schoombie J[1], Schoombie S[2], Connan M[2], Jones CW[3], Risi M[3], Craig KJ[1], Smith L[1], Ryan PG[3], Shepard ELC[4]*

[1] *Department of Mechanical and Aeronautical Engineering, University of Pretoria, Pretoria 0028, South Africa*

[2] *Department of Zoology, Marine Apex Predator Research Unit (MAPRU), Institute for Coastal and Marine Research, Nelson Mandela University, Gqeberha 6001, South Africa*

[3] *FitzPatrick Institute of African Ornithology, University of Cape Town, Rondebosch 7701. South Africa*

[4] *Department of Biosciences, Swansea University, Swansea SA2 8PP, UK*

*Corresponding author: Janine Schoombie, Janine.versteegh@gmail.com

This document contains the following

Literature cited

Schutgens M, Shaw JM, Ryan PG (2014) Estimating scavenger and search bias for collision fatality surveys of large birds on power lines in the Karoo, South Africa. Ostrich 85:39-45.

Appendix A: Carcass classification extended methods

Carcass condition classification

For the carcass surveys, it was necessary to develop a method to gauge carcass age from the level of decomposition. Similar methods have been used for other birds (e.g. powerline collision victims, Schutgens et al. 2014), but the rate of decomposition varies with bird size and the environmental conditions at the site (especially temperature and rainfall). A carcass with substantial flesh visible (fresh or dried), mostly intact skeleton and rhamphotheca (keratin sheath covering the bill) present was assumed to have died within the breeding season of a given survey and documented as "fresh". A carcass with only small amounts of dried flesh, little skin and the skeleton starting to come apart, but with the rhamphotheca still present, was assumed to have died during the previous breeding season and was documented as "intermediate". An intermediate carcass may also be partially covered by vegetation, with algae growing on feathers and bones. A carcass with only bones, minimal feathers, if any and the rhamphotheca absent was assumed to have died two or more breeding seasons ago and was documented as "old".

In September 2019, the carcass of an adult that was observed crashing into the Valley was moved close to the field hut to facilitate regular inspection. Photographs of the carcass were taken 1, 21, 50, 212, 418, 661 and 1047 days after death (Fig. S1). The same observer inspected the carcass 1-50 days after death. After 50 days (~7 weeks), the carcass remained mostly intact, with the wings separated from the body. Dried flesh and the rhamphotheca were clearly visible; skin and feathers still covered the wings' radius, ulna and hand bones. The skin on the feet had turned dark grey with some red/purple.

Inspection of the carcass 212, 418, 661 and 1047 days after the bird's death was done by four different observers, none of whom was informed of the time of death. After 212 days (~30 weeks or 7.5 months), the carcass remained largely intact, with algae visible on white feathers. Some dried flesh was still visible, particularly on wing bones, but the radius, ulna and wrist bones were all visible. The rhamphotheca had lighter patches, and the skin on the feet was pale orange. After 418 days (~60 weeks, October 2020), bones and some feathers were visible, with algae on bones and feathers. Smaller bones were partially hidden by vegetation. An independent observer noted the condition of this carcass as "intermediate" and determined the age from the partial rhamphotheca still visible. After 661 days (~94.5 weeks, June 2021), only a small pile of bones was visible, partially covered by vegetation. The rhamphotheca was absent, and an independent observer classified the carcass as "old". After 1047 days (~150 weeks, June of the 2021/22 breeding season), an independent observer noted only a few bones covered in algae and the rachises of a few flight feathers. Much of the carcass was covered by vegetation (Fig. S1).

These results confirm the adequacy of the classification system. It can take up to 3 years for a carcass to disappear and possibly even longer in areas with less vegetation.

Albatross age classification

Ageing of carcasses was based on colouration on rhamphotheca and plumage pattern. In fledglings, the entire rhamphotheca is mostly black, and the underwing feathers are dark grey. Adult grey-headed albatrosses have a yellow culminicorn, a yellow stripe along the ramicorn and white centres to the underwings. For carcasses where the rhamphotheca and feathers were absent, the age was recorded as

"unknown". This was true mostly for old carcasses, but in a few cases, the head of an intermediate carcass could not be located, and plumage colouration was unclear.

Fig. S1. Photographs taken of a grey-headed albatross carcass (a) 1 day, (b) 21 days, (c) 50 days, (d) 212 days, (e) 418 days, (f) 661 days and (g) 1047 days after death
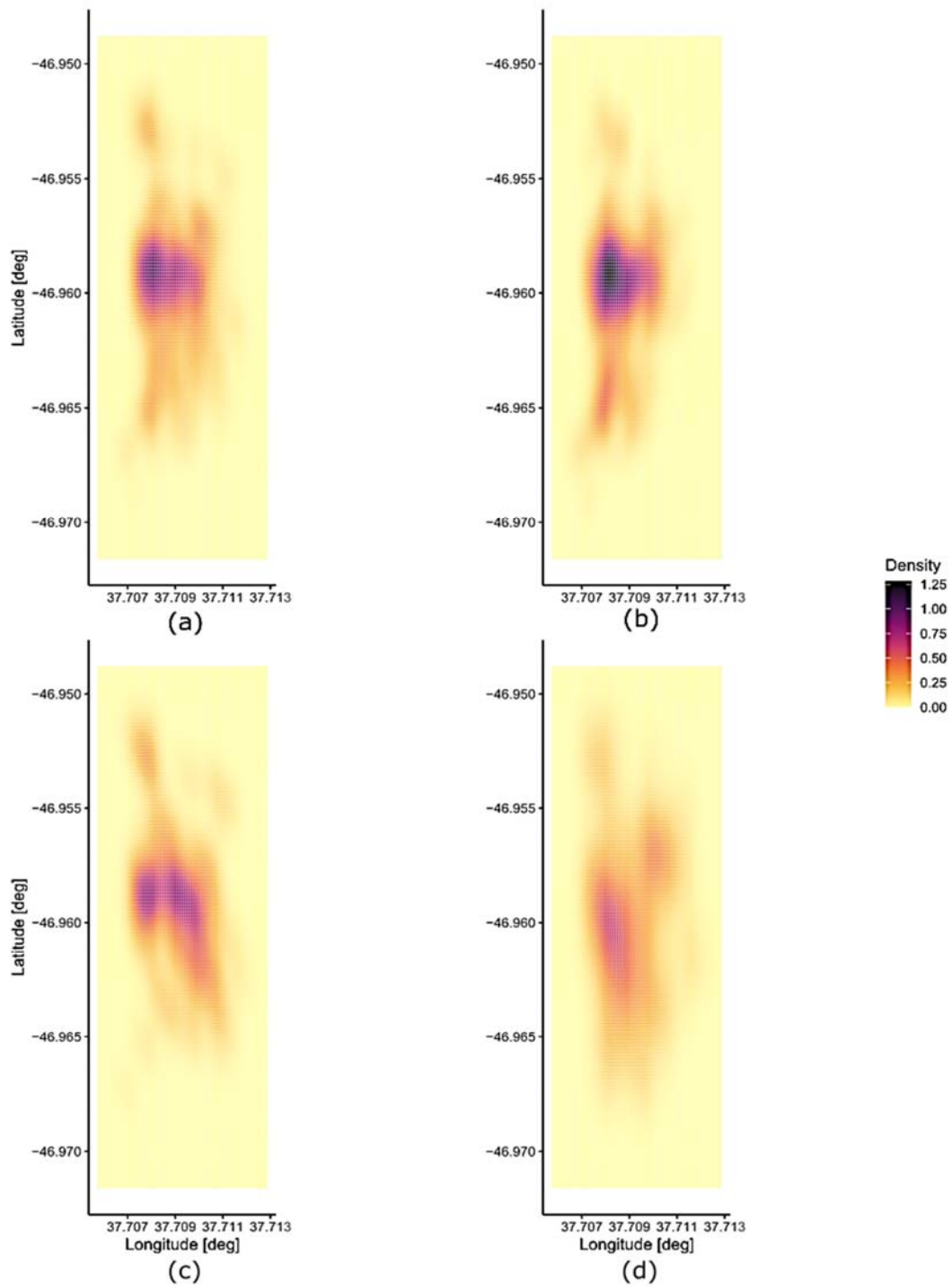
Fig. S2. Density of crash sites recorded in a c. 1 km^2 area in Santa Rosa Valley between October 2017 and June 2021, excluding live albatrosses. All birds (a, N = 513), adults (b, N = 222), fledglings (c, N = 194) and birds of unknown age (d, N = 97).
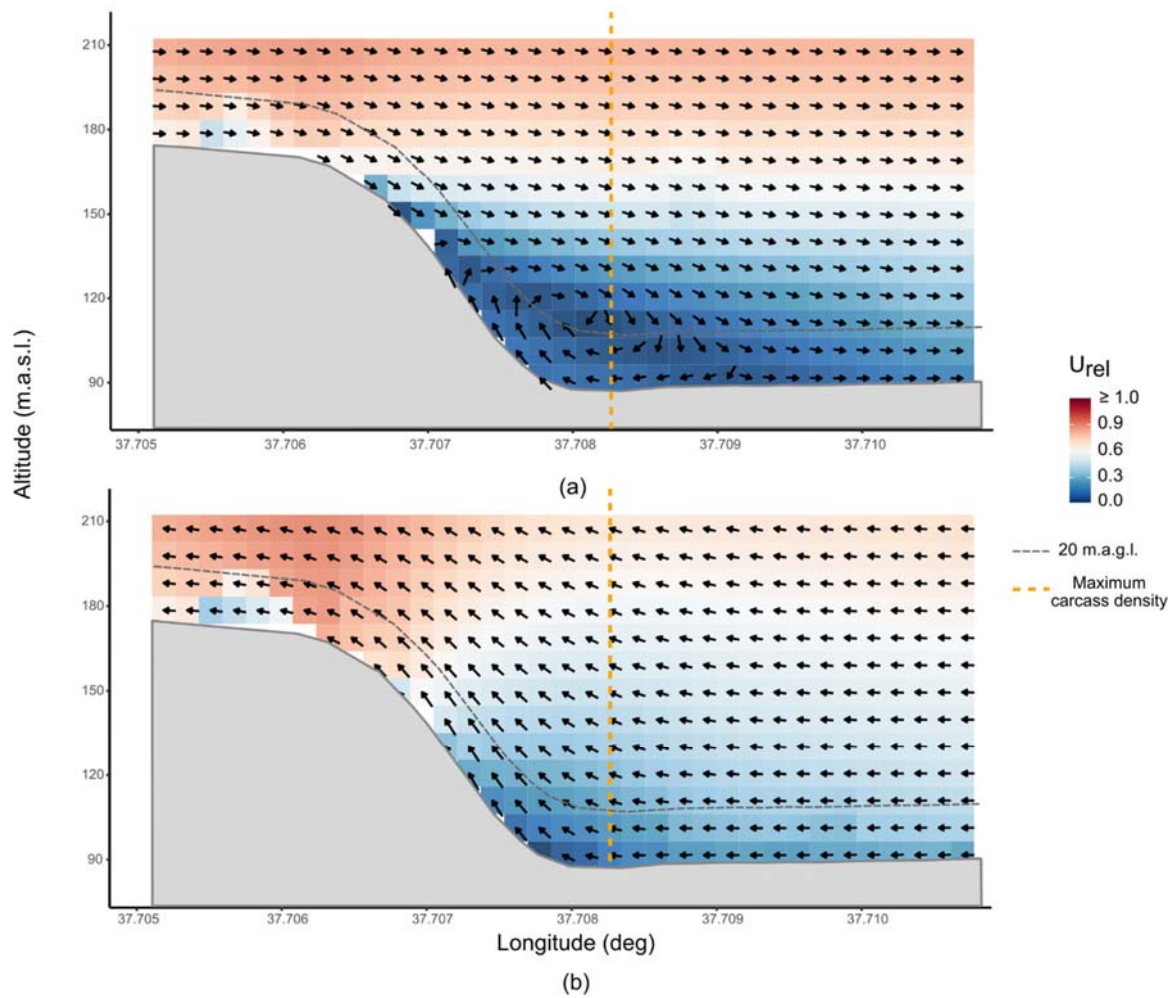
Fig. S3. Cross-section at a constant latitudinal line (-46.957°) corresponding to the maximum carcass density. Black arrows indicate two-dimensional vectors with the vertical and longitudinal velocity components with the background tiles coloured by the relative velocity (U_{rel}; velocity magnitude divided by U_{ref} = 3 m.s^{-1}), for westerly (a) and easterly (b) winds. The grey area is an approximation of the Ridge slope at this latitude, the grey dashed line is a constant 20 m.a.g.l line above the Valley and Ridge and the orange dashed line indicates the longitudinal line crossing the maximum carcass density.
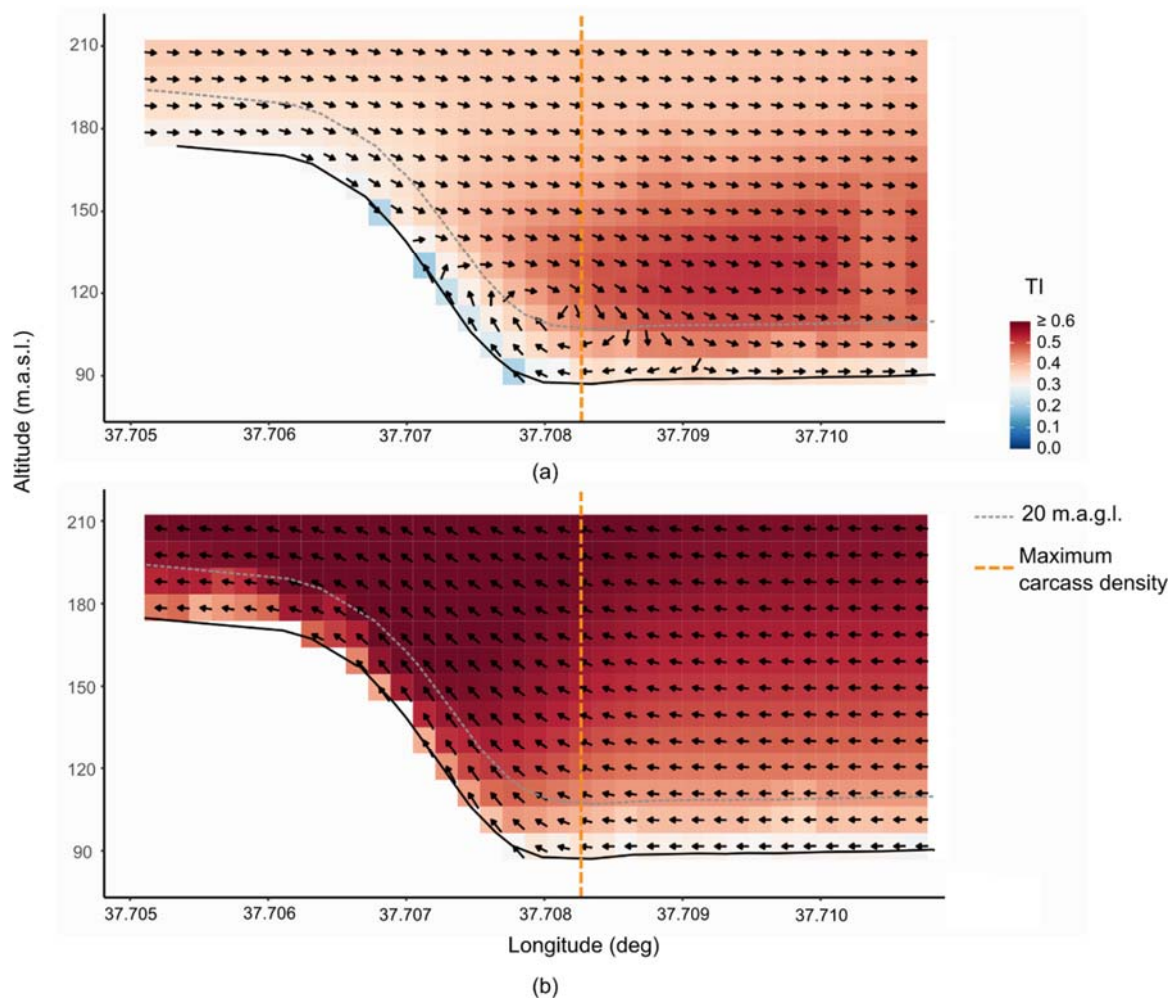
Fig. S4. Cross-section at a constant latitudinal line (-46.957°) corresponding to the maximum carcass density. Black arrows indicate two-dimensional vectors with the vertical and longitudinal velocity components with the background tiles coloured by the isotropic turbulence intensity (TI), for westerly (a) and easterly (b) winds. The grey area is an approximation of the Ridge slope at this latitude, the grey dashed line is a constant 20 m.a.g.l line above the Valley and Ridge and the orange dashed line indicates the longitudinal line crossing the maximum carcass density.
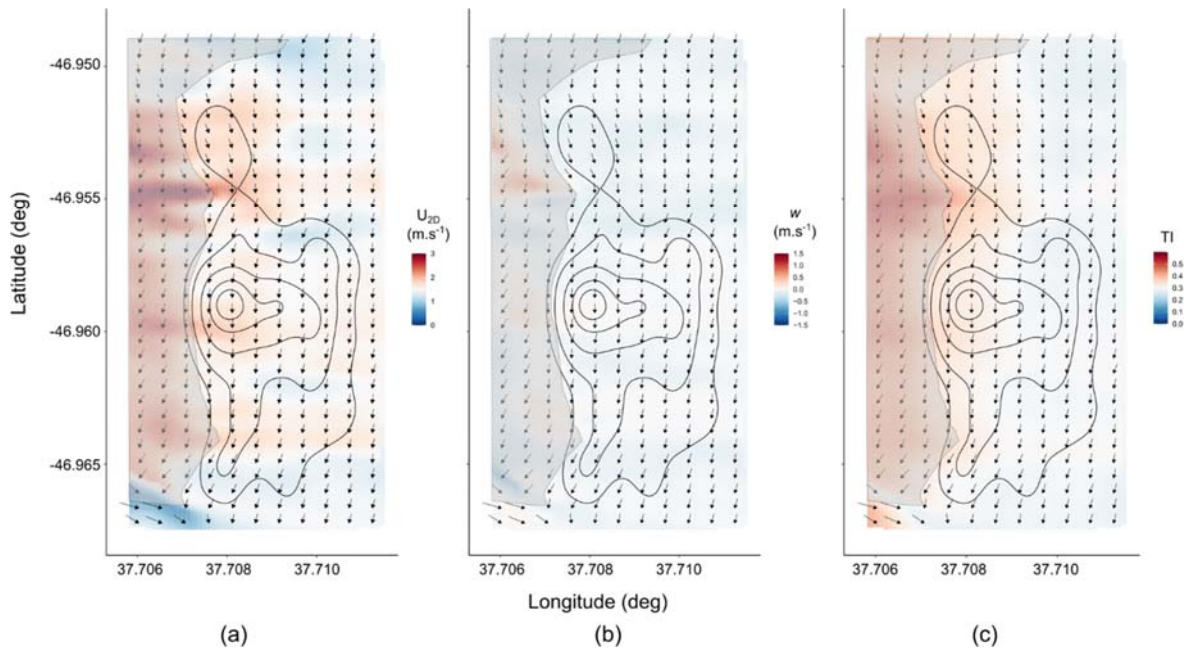
Fig. S5. Two-dimensional wind map, extracted at a constant 1 m.a.g.l. from numerical simulation of a Northerly wind ($\theta = 0°$ or $360°$) freestream condition over Marion Island. Crash site density contours (black, solid lines) are displayed with the outline of the base of the Ridge (semi-transparent grey area). Each grid point is denoted by an arrow indicating the wind direction (local wind direction) with backgrounds coloured by two-dimensional horizontal velocity magnitude (U_{2D}; a), the vertical wind component (w; b) and the isotropic turbulence intensity (TI; c).
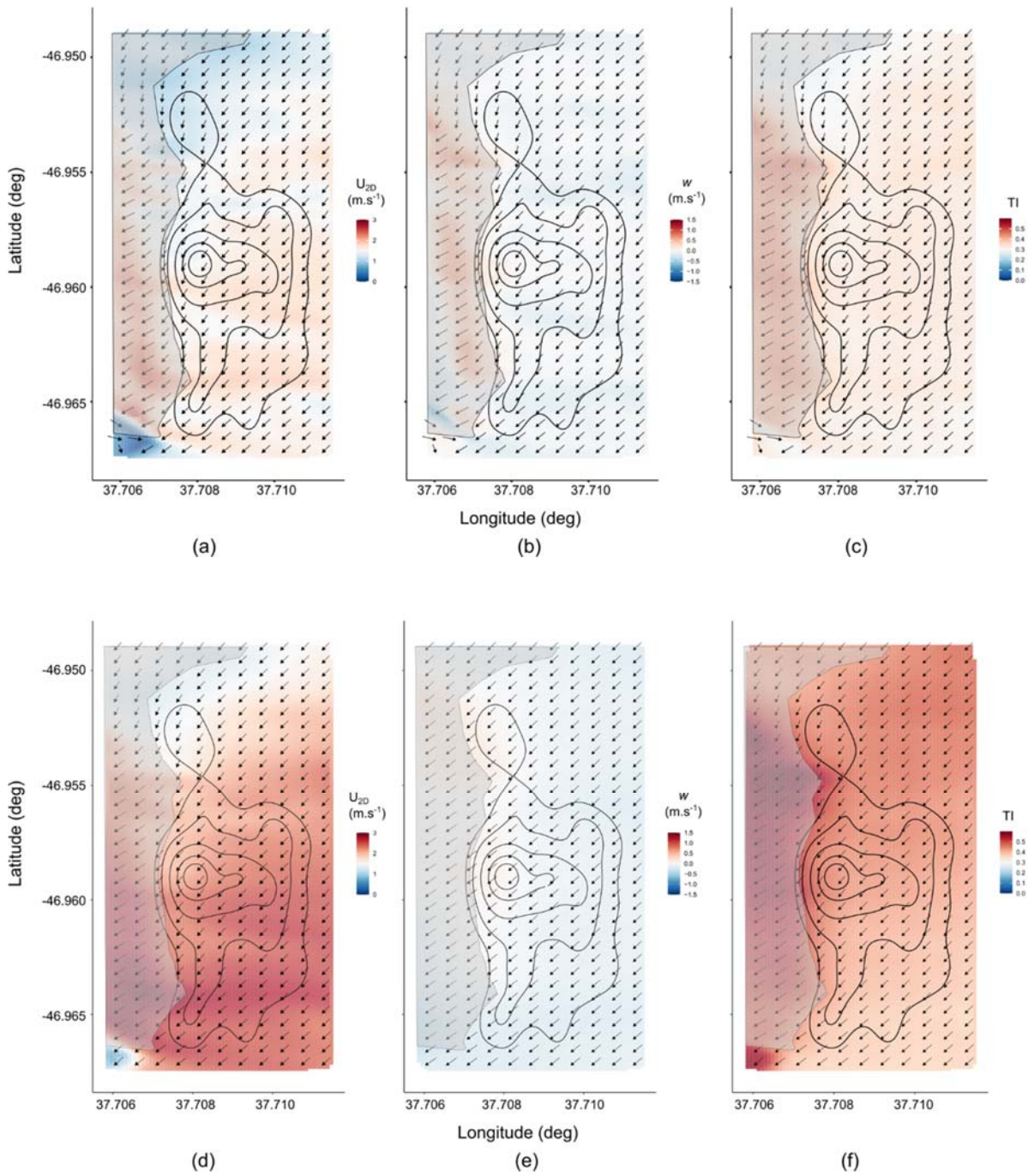
Fig. S6. Two-dimensional wind map, extracted at a constant 1 m.a.g.l. (a-c) and 20 m.a.g.l. (d-f) from numerical simulation of a north-easterly wind ($\theta = 45°$) freestream condition over Marion Island. Crash site density contours (black, solid lines) are displayed with the outline of the base of the Ridge (semi-transparent grey area).

Each grid point is denoted by an arrow indicating the wind direction (local wind direction) with backgrounds coloured by two-dimensional horizontal velocity magnitude (U_{2D}; a & d), the vertical wind component (w; b & e) and the isotropic turbulence intensity (TI; c & f).
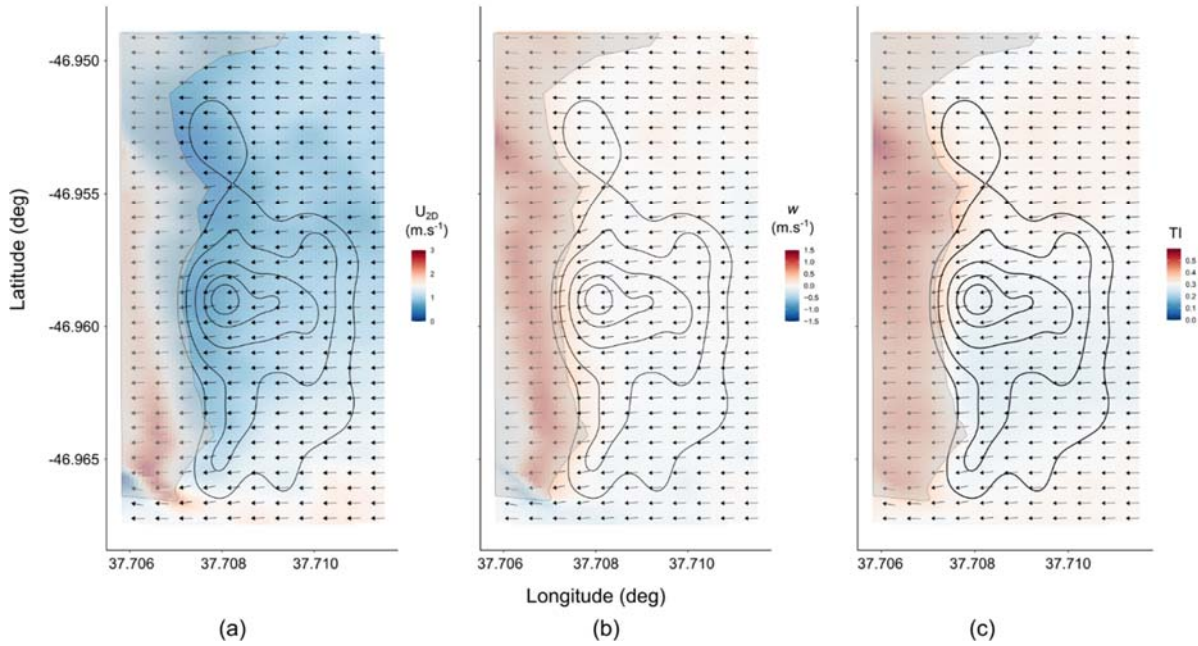

Fig. S7. Two-dimensional wind map, extracted at a constant 1 m.a.g.l. from numerical simulation of an easterly wind ($\theta = 90°$) freestream condition over Marion Island. Crash site density contours (black, solid lines) are displayed with the outline of the base of the Ridge (semi-transparent grey area). Each grid point is denoted by an arrow indicating the wind direction (local wind direction) with backgrounds coloured by two-dimensional horizontal velocity magnitude (U_{2D}; a), the vertical wind component (w; b) and the isotropic turbulence intensity (TI; c).
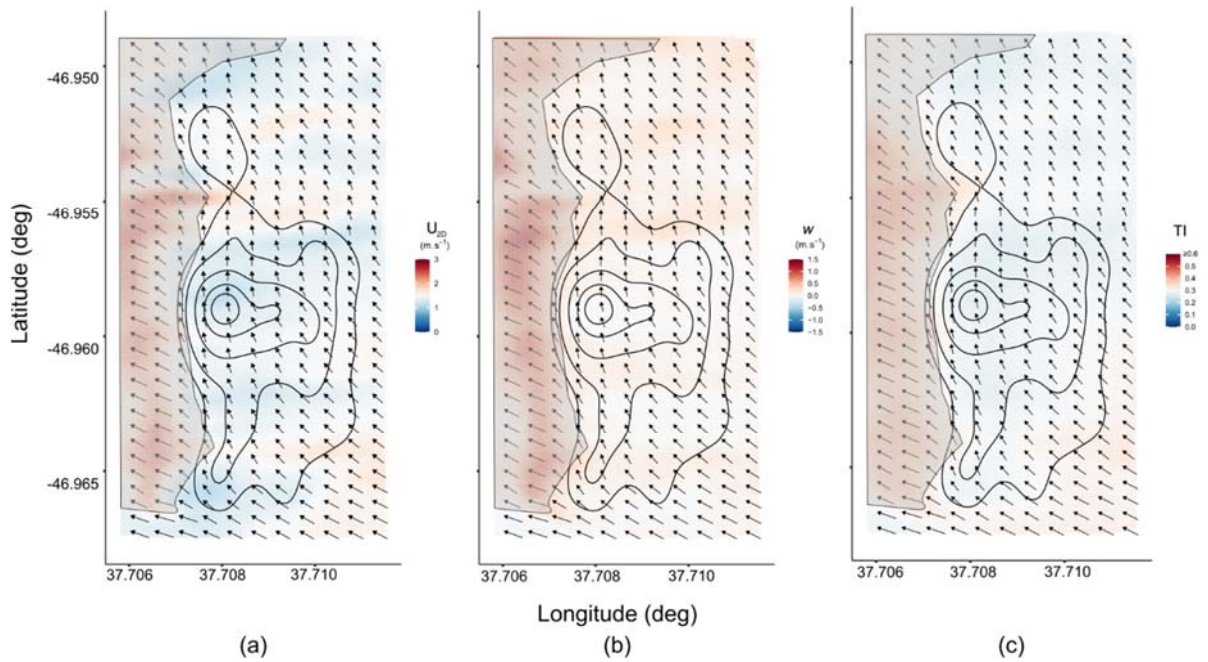
Fig. S8. Two-dimensional wind map, extracted at a constant 1 m.a.g.l. from numerical simulation of a south-easterly wind (θ = 135°) freestream condition over Marion Island. Crash site density contours (black, solid lines) are displayed with the outline of the base of the Ridge (semi-transparent grey area). Each grid point is denoted by an arrow indicating the wind direction (local wind direction) with backgrounds coloured by two-dimensional horizontal velocity magnitude (U_{2D}; a), the vertical wind component (w; b) and the isotropic turbulence intensity (TI; c)
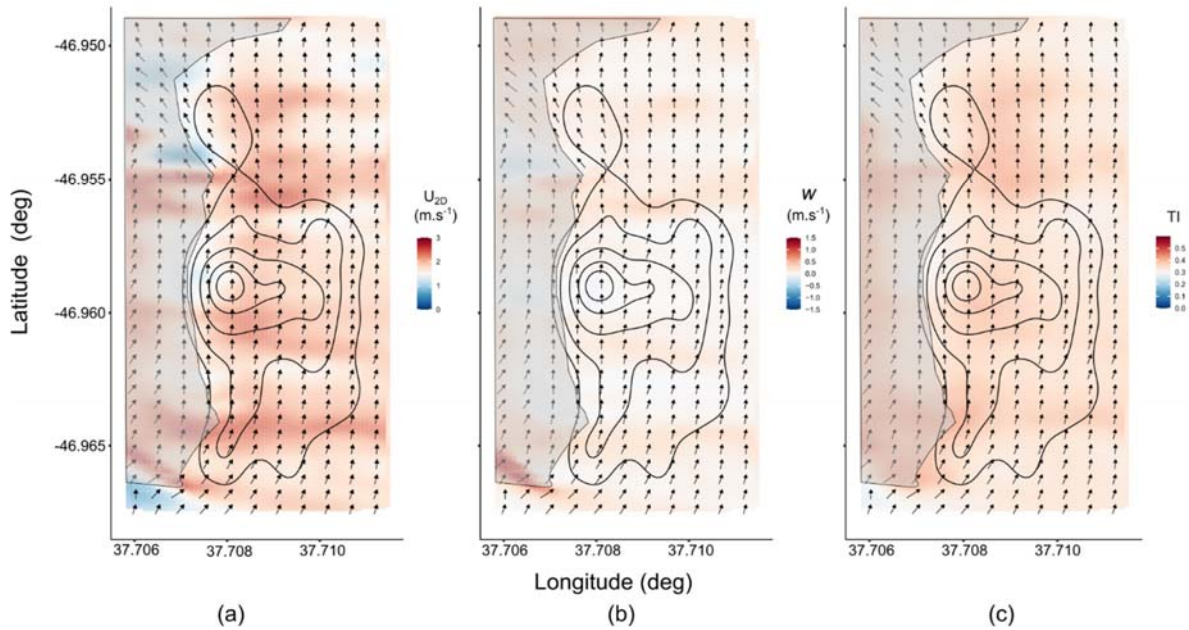
Fig. S9. Two-dimensional wind map, extracted at a constant 1 m.a.g.l. from numerical simulation of a southerly wind ($\theta = 180°$) freestream condition over Marion Island. Crash site density contours (black, solid lines) are displayed with the outline of the base of the Ridge (semi-transparent grey area). Each grid point is denoted by an arrow indicating the wind direction (local wind direction) with backgrounds coloured by two-dimensional horizontal velocity magnitude (U_{2D}; a), the vertical wind component (w; b) and the isotropic turbulence intensity (TI; c)
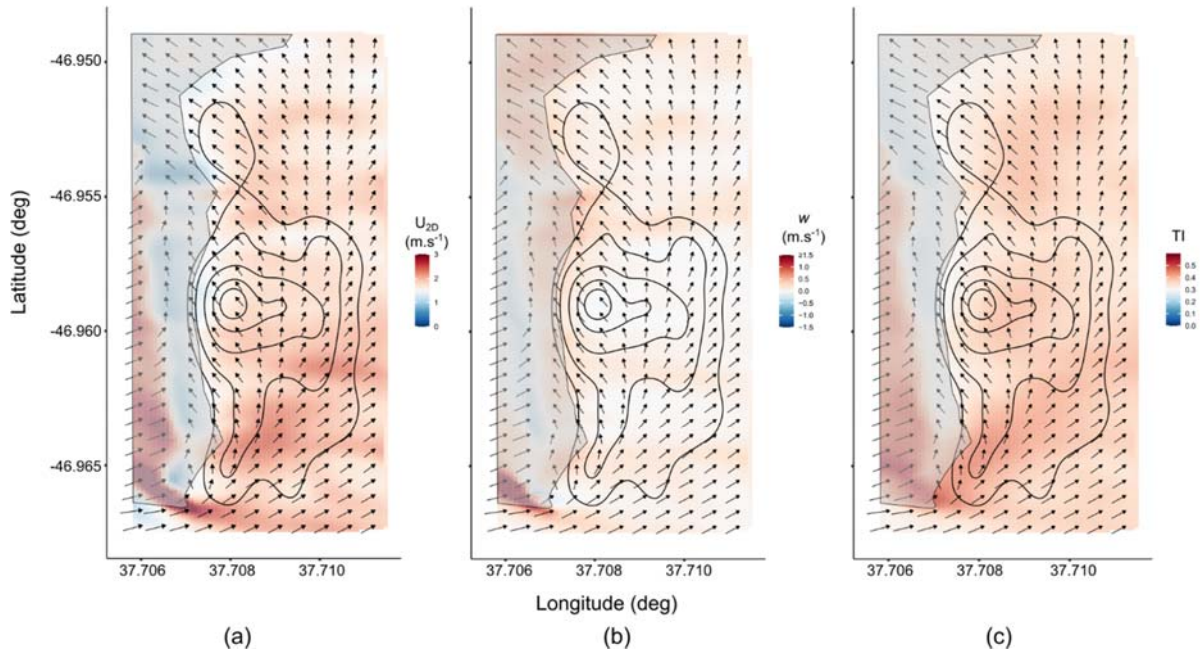
Fig. S10. Two-dimensional wind map, extracted at a constant 1 m.a.g.l. from numerical simulation of a south-westerly wind ($\theta = 225°$) freestream condition over Marion Island. Crash site density contours (black, solid lines) are displayed with the outline of the base of the Ridge (semi-transparent grey area). Each grid point is denoted by an arrow indicating the wind direction (local wind direction) with backgrounds coloured by two-dimensional horizontal velocity magnitude (U_{2D}; a), the vertical wind component (w; b) and the isotropic turbulence intensity (TI; c)
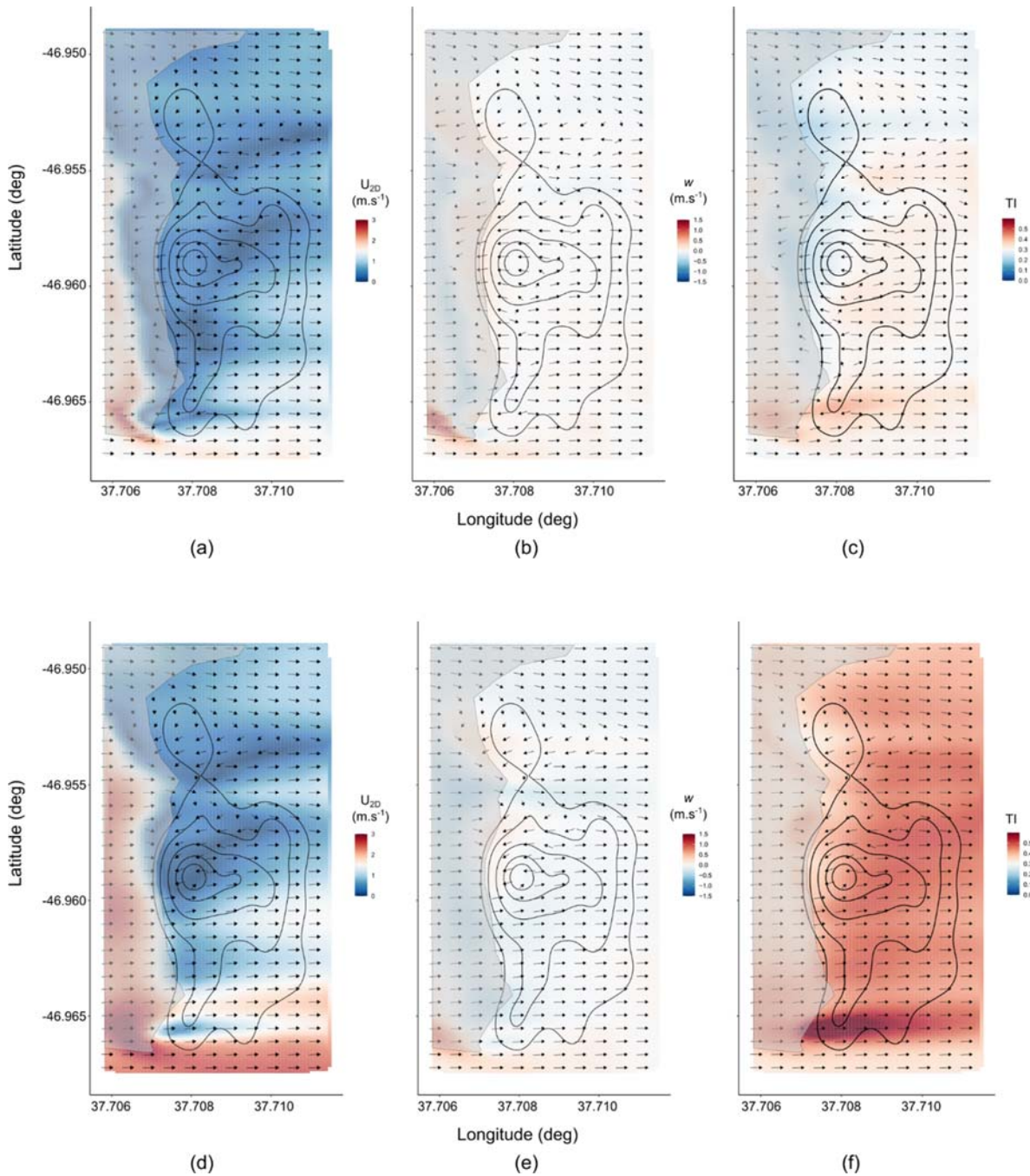
Fig. S11. Two-dimensional wind map, extracted at a constant 1 m.a.g.l. (a-c) and 20 m.a.g.l. (d-f) from numerical simulation of a westerly wind (θ = 270°) freestream condition over Marion Island. Crash site density contours (black, solid lines) are displayed with the outline of the base of the Ridge (semi-transparent grey area).

Each grid point is denoted by an arrow indicating the wind direction (local wind direction) with backgrounds coloured by two-dimensional horizontal velocity magnitude (U_{2D}; a & d), the vertical wind component (w; b & e) and the isotropic turbulence intensity (TI; c & f).
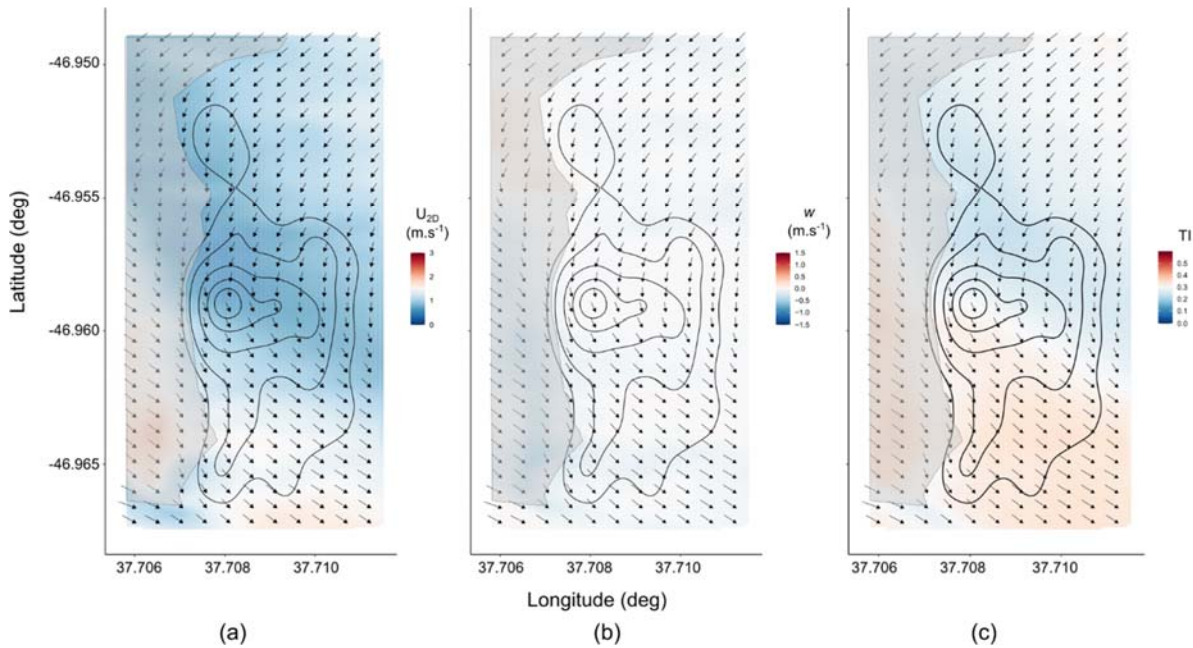

(a)   (b)   (c)

Fig. S12. Two-dimensional wind map, extracted at a constant 1 m.a.g.l. from numerical simulation of a north-westerly wind ($\theta = 315°$) freestream condition over Marion Island. Crash site density contours (black, solid lines) are displayed with the outline of the base of the Ridge (semi-transparent grey area). Each grid point is denoted by an arrow indicating the wind direction (local wind direction) with backgrounds coloured by two-dimensional horizontal velocity magnitude (U_{2D}; a), the vertical wind component (w; b) and the isotropic turbulence intensity (TI; c).